

Phylogenetic analyses and morphological characters reveal two new species of *Ganoderma* from Yunnan province, China

Jun He^{1,2}, Zong-Long Luo¹, Song-Ming Tang^{2,3,4},
Yong-Jun Li², Shu-Hong Li², Hong-Yan Su¹

1 College of Agriculture and Biological Sciences, Dali University, Dali 671003, Yunnan, China **2** Institute of Biotechnology and Germplasm Resources, Yunnan Academy of Agricultural Sciences, Kunming 650223, China

3 Center of Excellence in Fungal Research, Mae Fah Luang University, Chiang Rai 57100, Thailand **4** School of science, Mae Fah Luang University, Chiang Rai 57100, Thailand

Corresponding authors: Shu-Hong Li (shuhongfungi@126.com), Hong-Yan Su (suhongyan16@163.com)

Academic editor: Bao-Kai Cui | Received 10 June 2021 | Accepted 17 October 2021 | Published 12 November 2021

Citation: He J, Luo Z-L, Tang S-M, Li Y-J, Li S-H, Su H-Y (2021) Phylogenetic analyses and morphological characters reveal two new species of *Ganoderma* from Yunnan province, China. MycoKeys 84: 141–162. <https://doi.org/10.3897/mycokeys.84.69449>

Abstract

Ganoderma dianzhongense sp. nov. and *G. esculentum* sp. nov. are proposed as two new species based on both phenotypic and genotypic evidences. *Ganoderma dianzhongense* is characterized by the stipitate basidiomata, laccate and oxblood red pileus, gray white pore surface, duplex context and broadly ellipsoid basidiospores ($9.0\text{--}12.5 \times 6.5\text{--}9.0 \mu\text{m}$) with coarse interwall pillars. *Ganoderma esculentum* is characterized by its basidiomata with slender stipe, white pore surface, homogeneous pileus context, and slightly truncate, narrow basidiospores ($8.0\text{--}12.5 \times 5.0\text{--}8.0 \mu\text{m}$). Phylogenetic analyses were carried out based on the internal transcribed spacer (ITS), translation elongation factor 1- α (TEF1- α) and the second subunit of RNA polymerase II (RPB2) sequence data. The illustrations and descriptions for the new taxa are provided.

Keywords

Ganodermataceae, novel species, phylogeny, taxonomy

Introduction

Ganodermataceae was introduced by Donk (1948) which belongs to Polyporales and the latest studies indicated that it is a monophyletic group (Costa-Rezende et al. 2020). Currently, eleven genera viz. *Amauroderma* Murril, *Amaurodermellus* Costa-Rezende, *Cristataspora* Costa-Rezende, *Foraminispora* Robledo, Costa-Rezende & Drechsler-Santos, *Furtadoa* Costa-Rezende, Robledo & Drechsler-Santos, *Ganoderma* P. Karst., *Haddowia* Steyaert, *Humphreya* Steyaert, *Magoderna* (Murrill) Steyaert, *Sanguinoderma* Y.F. Sun, D.H. Costa & B.K. Cui and *Tomophagus* Murrill are accepted in Ganodermataceae and supported by morphology and phylogeny (Steyaert 1972; Furtado 1981; Corner 1983; Zhao et al. 2000; Ryvarden 2004; Thametal 2012; Costa-Rezende et al. 2017; Costa-Rezende et al. 2020; Sun et al. 2020).

Ganoderma P. Karst (Ganodermataceae, Polyporales) was introduced to accommodate a laccate and stipitate fungus, *Ganoderma lucidum* (Curtis) P. Karst (Karsten 1881). *Ganoderma* is characterized by double-walled basidiospores with inter-wall protuberances (Karsten 1881; Moncalvo and Ryvarden 1997). There are 462 records in the Index Fungorum (<http://www.Indexfungorum.org/>; accessed date: 7 October 2021) and 506 records in MycoBank (<http://www.mycobank.org/>; accessed date: 7 October 2021). *Ganoderma* is one of the most taxonomically scrutinized genera among the Ganodermataceae and even in Polyporales (Richter et al. 2015; Costa-Rezende et al. 2020). Most *Ganoderma* species are wood decomposers, found in all temperate and tropical regions (Pilotti et al. 2004; Cao et al. 2012; Zhou et al. 2015).

Ganoderma has long been regarded as one of the most important medicinal fungi in the world (Paterson 2006); they have been used as medicine for over two millennia in China (Dai et al. 2009). Several *Ganoderma* species are known to be prolific sources of highly active bioactive compounds, especially polysaccharides, protein, sterols, and triterpenoids (Ahmadi and Riazipour 2007; Chan et al. 2007). These compounds are known to possess extensive therapeutic properties, such as antioxidant, antitumor, and antiviral agents, and improve sleep function (De Silva et al. 2013).

Species diversity of *Ganoderma* is abundant in China and more than 30 species have been described (Zhao et al. 2000; Wang et al. 2009; Cao et al. 2012; Li et al. 2015; Xing et al. 2016; Hapuarachchi et al. 2018; Liu et al. 2019; He et al. 2019; Wu et al. 2020). Yunnan province is considered as one of the hot-spots for studying biodiversity of polypores, and some new *Ganoderma* species have been described (Zhao 1989; Wang et al. 2010; Cao and Yuan 2013).

During our investigation into the diversity of *Ganoderma* in Yunnan province, several specimens of *Ganoderma* were collected from central and southern Yunnan. Phylogenetic analysis showed that the seven collections formed two distinct lineages and can be recognized as new species, hence two new species, namely *G. dianzhongense* and *G. esculentum* are introduced based on morphology and phylogeny.

Materials and methods

Sample collection

Seven *Ganoderma* specimens were collected during the rainy season from July 2016 to August 2019 in Yunnan Province of China. The samples were then photographed and transported back to the laboratory where their fresh macroscopic details were described. The specimens were deposited in the herbarium of Kunming Institute of Botany Academia Sinica (KUN-HKAS).

Morphological studies

Macro-morphological characters were described based on fresh material field notes, and the photographs provided here. Color codes are from Kornerup and Wanscher (1978). Micro-morphological data were obtained from the dried specimens and observed by using a microscope following Li et al. (2015). Sections were studied at magnification of up to 1000 \times using a NiKon E400 microscope and phase contrast illumination. Microscopic features and measurements were made from slide preparations stained with 5% potassium hydroxide (KOH) and 2% Melzer's reagent. Basidiospore features, hyphal system, color, sizes and shapes were recorded and photographed. Measurements were made using the Image Frame work v.0.9.7 to represent variation in the size of basidiospores, 5% of measurements were excluded from each end of the range and extreme values are given in parentheses.

The following abbreviations are used: IKI = Melzer's reagent, IKI- = neither amyloid nor dextrinoid, KOH = 5% potassium hydroxide, CB = Cotton Blue, CB+ = Cyanophilous (Xing et al. 2018). The abbreviation for basidiospores measurements (n/m/p) denote "n" basidiospores measured from "m" basidiomata of "p" specimens. Basidiospore dimensions (and "Q" values) are given as (a) b-av-c (d), where "a" represents the minimum, "d" the biggest, "av" the average "b" and "c" covers a minimum of 90% of the values. "Q", the length/width ratio of a spore in side view, and "Q_m" for the average of all basidiospores \pm standard deviation (Wang et al. 2015).

DNA extraction, PCR amplification, and sequencing

Total genomic DNA was extracted from dried pieces of pileus with tubes with modified CTAB protocol Doyle (1987). The genes ITS, TEF1- α and RPB2 were amplified by polymerase chain reaction (PCR) technique. The primers ITS1F / ITS4, TEF1-983 / TEF1-1567, and RPB2-6f / fRPB2-7cR were used to amplify the ITS, TEF1- α , RPB2 region, respectively (White et al. 1990; Liu et al. 1999; Matheny et al. 2007). PCR reactions (25 μ L) contained mixture: 2.5 μ L PCR reaction buffer, 2.5 μ L 0.2% BSA, 2 μ L dNTP (2.5 mm), 0.5 μ L each of primer, 0.2 μ L 5 U/ μ L Taq DNA polymerase, 1–1.5 μ L DNA solution and 16 μ L sterilized distilled H₂O. The PCR cycling for ITS was as follows: initial denaturation at 94 °C for 5 min, followed by 35 cycles at

94 °C for 30 sec, 53 °C for 30 sec and 72 °C for 50 sec and a final extension of 72 °C for 10 min. The PCR cycling for TEF1- α was as follows: initial denaturation at 94 °C for 5 min, followed by 35 cycles at 94 °C for 30 sec, 55 °C for 30 sec and 72 °C for 50 sec and a final extension of 72 °C for 10 min. The PCR cycling for RPB2 was as follows: initial denaturation at 94 °C for 5 min, followed by 35 cycles at 94 °C for 30 sec, 50 °C for 30 sec and 72 °C for 50 sec and a final extension of 72 °C for 10 min. The PCR products were visualized via UV light after electrophoresis on 1% agarose gels stained with ethidium bromide. Successful PCR products were sent to Sangon Biotech Limited Company (Shanghai, China), using forward PCR primers. When sequences have heterozygous INDELS or ambiguous sites, samples were sequenced bidirectionally to make contigs of the amplified regions or verify the ambiguous sites (Wang et al. 2015). Raw DNA sequences were assembled and edited in Sequencher 4.1.4 and the assembled DNA sequences were deposited in GenBank (Table 1).

Sequencing and sequence alignment

Sequence data of three partial loci Internal transcribed spacer region (ITS), RNA polymerase II subunit 2 (RPB2), and translation elongation factor 1-alpha (TEF1- α) were used in the phylogenetic analyses. Besides the sequences generated from this study, other reference sequences were selected from GenBank for phylogenetic analyses (Table 1). Sequences were aligned using the online version of MAFFT v.7 (<http://mafft.cbrc.jp/alignment/server/>) (Katoh and Standley 2013) and adjusted using BioEdit v.7.0.9 by hand (Hall 1999) to allow maximum alignment and minimize gaps. Ambiguous regions were excluded from the analyses and gaps were treated as missing data. The phylogeny website tool “ALTER” (Glez-Peña et al. 2010) was used to convert the alignment fasta file to Phylip format for RAxML analysis and AliView and PAUP 4.0b 10 were used to convert the alignment fasta file to a Nexus file for Bayesian analysis (Swofford 2003). Phylogenetic analyses were obtained from Maximum Likelihood (ML) and Bayesian analysis (BI).

Molecular phylogenetic analyses

The maximum likelihood (ML) and Bayesian inference (BI) methods were used to analyze the combined dataset of ITS, TEF1- α and RPB2 sequences. Maximum likelihood analysis was conducted with RAxML-HPC2 on the CIPRES Science Gateway (Miller et al. 2010), involved 100 ML searches; all model parameters were estimated by the program. The ML bootstrap values (ML-BS) were obtained with 1000 rapid bootstrapping replicates. Maximum likelihood bootstrap values (ML) equal to or greater than 70% are given above each node (Figure 1).

Bayesian analysis was performed with MrBayes v3.2 (Ronquist et al. 2012), with the best-fit model of sequence evolution estimated with MrModeltest 2.3 (Nylander et al. 2008) to evaluate posterior probabilities (PP) (Rannala and Yang 1996; Zhaxybayeva and Gogarten 2002) by Markov Chain Monte Carlo (MCMC) sampling. Six simultaneous Markov chains were run for 10,000,000 generations, trees were sampled every 500th generation, and 2,000 trees were obtained. The first 5000 trees, represent-

Table 1. Species, specimens, geographic origin and GenBank accession numbers of sequences used in this study.

Species	Voucher/strain	Origin	GenBank accession numbers			Reference
			ITS	TEF1- α	RPB2	
<i>Ganoderma aridicola</i>	Dai 12588 (Type)	South Africa	KU572491	KU572502	—	Xing et al. 2016
<i>G. adpersum</i>	GACP15061220	Thailand	MK345425	MK371431	MK371437	Hapuarachchi et al. 2019
	MFLU 19-2178	Thailand	MN396653	MN423149	MN423114	Luangharn et al. 2021
<i>G. angustisporum</i>	Cui 13817 (Type)	Fujian, China	MG279170	MG367563	MG367507	Xing et al. 2018
	Cui 14578	Guangdong, China	MG279171	MG367564	—	Xing et al. 2018
<i>G. austral</i>	CMW 47785	South Africa	MH571686	MH567276	—	Tchoumi et al. 2018
	CMW 48146	South Africa	MH571685	MH567283	—	Tchoumi et al. 2018
<i>G. austroafricanum</i>	CBSI38724 (Type)	South Africa	KM507324	—	—	Coetze et al. 2015
<i>G. aff. austroafricanum</i>	CMW25884	South Africa	MH571693	MH567296	—	Tchoumi et al. 2019
<i>G. bambusicola</i>	Wu 1207-151 (Type)	Taiwan, China	MN957781	LC517941	LC517944	Wu et al. 2020
	Wu 1207-152	Taiwan, China	MN957782	LC517942	LC517945	Wu et al. 2020
	Wu 1207-153	Taiwan, China	MN957783	LC517943	LC517946	Wu et al. 2020
<i>G. boninense</i>	WD 2028	Japan	KJ143905	KJ143924	KJ143964	Zhou et al. 2015
	WD 2085	Japan	KJ143906	KJ143925	KJ143965	Zhou et al. 2015
<i>G. calidophilum</i>	MFLU 19-2174	Yunnan, China	MN398337	—	—	Luangharn et al. 2021
	H36	Yunnan, China	MW750241 [*]	MW838997 [*]	MW839003 [*]	this study
<i>G. carnosum</i>	MJ 21/08	Czech R, Europe	KU572492	—	—	Xing et al. 2016
	JV 8709/8	Czech R, Europe	KU572493	—	—	Xing et al. 2016
<i>G. carocalcareus</i>	DMC 322 (Type)	Cameroon	EU089969	—	—	Douanla and Langer 2009
	DMC 513	Cameroon	EU089970	—	—	Douanla and Langer 2009
<i>G. casuarinicola</i>	Dai 16336 (Type)	Guangdong, China	MG279173	MG367565	MG367508	Xing et al. 2018
	Dai 16339	Guangdong, China	MG279176	MG367568	MG367511	Xing et al. 2018
<i>G. curtisii</i>	CBS 100131	NC, USA	JQ781848	KJ143926	KJ143966	Zhou et al. 2015
	CBS 100132	NC, USA	JQ781849	KJ143927	KJ143967	Zhou et al. 2015
<i>G. destructans</i>	CBS 139793 (Type)	South Africa	NR132919	—	—	Coetze et al. 2015
	Dai 16431	South Africa	MG279177	MG367569	MG367512	Xing et al. 2018
<i>G. dunense</i>	CMW42157 (Type)	South Africa	MG020255	MG020227	—	Tchoumi et al. 2019
	CMW42150	South Africa	MG020249	MG020228	—	Tchoumi et al. 2019
<i>G. ecuadoriense</i>	ASL799 (Type)	Ecuador	KU128524	—	—	Crous et al. 2016
	PMC126	Ecuador	KU128525	—	—	Crous et al. 2016
<i>G. eickeri</i>	CMW 49692 (Type)	South Africa	MH571690	MH567287	—	Tchoumi et al. 2019
	CMW 50325	South Africa	MH571689	MH567290	—	Tchoumi et al. 2019
<i>G. ellipoideum</i>	GACP1408966 (Type)	Hainan, China	MH106867	—	—	Hapuarachchi et al. 2018
	GACP14081215	Hainan, China	MH106886	—	—	Hapuarachchi et al. 2018
<i>G. enigmaticum</i>	Dai 15970	Africa	KU572486	KU572496	MG367513	Xing et al. 2016
	Dai 15971	Africa	KU572487	KU572497	MG367514	Xing et al. 2016
<i>G. esculentum</i>	L4935 (Type)	Yunnan, China	MW750242 [*]	MW838998 [*]	MW839004 [*]	this study
	L4946	Yunnan, China	MW750243 [*]	MW838999 [*]	—	this study
<i>G. flexipes</i>	Wei 5494	Hainan, China	JN383979	—	—	Cao and Yuan 2013
	MFLU 19-2198	Yunnan, China	MN398340	—	—	Luangharn et al. 2021
<i>G. gibbosum</i>	MFLU 19-2176	Thailand	MN396311	—	MN423118	Luangharn et al. 2021
	MFLU 19-2190	Laos	MN396310	—	MN423117	Luangharn et al. 2021
<i>G. heobnelianum</i>	Dai 11995	Yunnan, China	KU219988	MG367550	MG367497	Song et al. 2016
	Cui 13982	Guangxi, China	MG279178	MG367570	MG367515	Xing et al. 2018
<i>G. hochiminense</i>	MFLU 19-2224 (Type)	Vietnam	MN398324	MN423176	—	Luangharn et al. 2021
	MFLU 19-2225	Vietnam	MN396662	MN423177	—	Luangharn et al. 2021
<i>G. knysnamense</i>	CMW 47755 (Type)	South Africa	MH571681	MH567261	—	Tchoumi et al. 2019
	CMW 47756	South Africa	MH571684	MH567274	—	Tchoumi et al. 2019
<i>G. leucocontextum</i>	GDGM 44303	Xizang, China	KJ027607	—	—	Li et al. 2015
	GDGM 44305	Xizang, China	KJ027609	—	—	Li et al. 2015
<i>G. lingzhi</i>	Cui 9166	China	KJ143907	JX029974	JX029978	Cao et al. 2012
	Dai 12574	Liaoning, China	KJ143908	JX029977	JX029981	Cao et al. 2012
<i>G. lobatum</i>	JV 1008/31	USA	KF605671	MG367553	MG367499	Xing et al. 2018
	JV 1008/32	USA	KF605670	MG367554	MG367500	Xing et al. 2018

<i>G. lucidum</i>	K 175217 MT 26/10	UK Czech Republic	KJ143911 KJ143912	KJ143929 KJ143930	KJ143971	Zhou et al. 2015
<i>G. martinicense</i>	231NC 246TX	NC, USA TX, USA	MG654182 MG654185	MG754736 MG754737	— MG754858	Loyd et al. 2018 Loyd et al. 2018
<i>G. mbrekobenum</i>	UMN7-3 GHA (Type) UMN7-4 GHA	Ghana Ghana	KX000896 KX000898	— —	— —	Crous et al. 2016 Crous et al. 2016
<i>G. mexicanum</i>	MUCL 49453 SW17 MUCL 55832	Martinique Martinique	MK531811 MK531815	MK531825 MK531829	MK531836 MK531839	Cabarroi-Hernández et al. 2019 Cabarroi-Hernández et al. 2019
<i>G. mizoramense</i>	UMN-MZ4 (Type) UMN-MZ5	India India	KY643750 KY643751	— —	— —	Crous et al. 2017 Crous et al. 2017
<i>G. multipileum</i>	CWN 04670 Dai 9447	Taiwan, China Hainan, China	KJ143913 KJ143914	KJ143931 —	KJ143972 KJ143973	Zhou et al. 2015 Zhou et al. 2015
<i>G. multiplicatum</i>	SPC9 URM 83346	Brazil Brazil	KU569553 JX310823	— —	— —	Bolaños et al. 2016 Bolaños et al. 2016
<i>G. mutabile</i>	CLZhao 982 Yuan 2289(Type)	Yunnan, China Yunnan, China	MG231527 JN38977	— —	— —	GenBank Cao and Yuan 2013
<i>G. myanmarensis</i>	MFLU 19-2167 (Type) MFLU 19-2169	Myanmar Myanmar	MN396329 MN396330	— —	— —	Luangharn et al. 2021 Luangharn et al. 2021
<i>G. nasalanense</i>	GACP17060211 (Type) GACP17060212	Laos Laos	MK345441 MK345442	— —	— —	Hapuarachchi et al. 2019
<i>G. neojaponicum</i>	FFPRI WD-1285 FFPRI WD-1532	Tokyo, Japan Chiba, Japan	MN957784 MN957785	— —	— —	Wu et al. 2020 Wu et al. 2020
<i>G. orbiforme</i>	Cui 13918 Cui 13880	Hainan, China Hainan, China	MG279186 MG279187	MG367576 MG367577	MG367522 MG367523	Xing et al. 2018 Xing et al. 2018
<i>G. parvulum</i>	MUCL 47096 MUCL 52655	Cuba French Guiana	MK554783 MK554770	MK554721 MK554717	MK554742 MK554755	Cabarroi-Hernández et al. 2019 Cabarroi-Hernández et al. 2019
<i>G. philippii</i>	Cui 14443 Cui 14444	Hainan, China Hainan, China	MG279188 MG279189	MG367578 MG367579	MG367524 MG367525	Xing et al. 2018 Xing et al. 2018
<i>G. resinaceum</i>	Rivoire 4150 CBS 19476	France, Europe Netherlands, Europe	KJ143915 KJ143916	— KJ143934	— —	Zhou et al. 2015 Zhou et al. 2015
<i>G. ryvardenii</i>	HKAS 58053 (Type) HKAS 58054	South Africa South Africa	HM138670 HM138671	— —	— —	Kinge et al. 2011 Kinge et al. 2011
<i>G. sessile</i>	111TX 113FL	TX, USA FL, USA	MG654306 MG654307	MG754747 MG754748	MG754866 MG754867	Loyd et al. 2018 Loyd et al. 2018
<i>G. shanxiense</i>	BJTC FM423(Type) HSA 539	Shanxi, China Shanxi, China	MK764268 MK764269	MK783937 —	MK783940 MK789681	Liu et al. 2019 Liu et al. 2019
<i>G. sichuanense</i>	HMAS42798 (Type) Cui 7691	Sichuan, China Guangdong, China	JQ781877 JQ781878	— —	— —	Cao et al. 2012 Cao et al. 2012
<i>G. sinense</i>	Wei 5327 Cui 13835	Hainan, China Hainan, China	KF494998 MG279193	KF494976 MG367583	MG367529 MG367530	Xing et al. 2018 Xing et al. 2018
<i>G. steyaertanum</i>	MEL:2382783 6 WN 20B	Australia Indonesia	KP012964 KJ654462	— —	— —	GenBank Glen et al. 2014
<i>G. thailandicum</i>	HKAS 104640 (Type) HKAS 104641	Thailand Thailand	MK848681 MK848682	MK875829 MK875830	MK875831 MK875832	Luangharn et al. 2019 Luangharn et al. 2019
<i>G. tropicum</i>	He 1232 HKAS 97486	Guangxi, China Thailand	KF495000 MH823539	KF494975 —	MG367531 MH883621	Xing et al. 2016 Luangharn et al. 2021
<i>G. tsugae</i>	UMNNMI20 UMNNMI30	MI, USA MI, USA	MG654324 MG654326	MG754764 MH025362	— MG754871	Loyd et al. 2018 Loyd et al. 2018
<i>G. tuberculosum</i>	GVL-21 GVL-40	Veracruz, Mexico Veracruz, Mexico	MT232639 MT232634	— —	— —	Espinosa-García et al. 2021 Espinosa-García et al. 2021
<i>G. weberianum</i>	CBS 128581 CBS 219.36	Taiwan, China Philippines	MK603805 MK603804	MK636693 MK611974	MK611971 MK611972	Cabarroi-Hernández et al. 2019 Cabarroi-Hernández et al. 2019

<i>G. wiirens</i>	UMN-21-GHA (Type) UMN-20-GHA	Ghana Ghana	KT952363 KT952361	— —	— —	Crous et al. 2015 Crous et al. 2015
<i>G. dianzhongense</i>	L4331(Type) L4230 L4737 L4759 L4969	Yunnan, China Yunnan, China Yunnan, China Yunnan, China Yunnan, China	MW750237* MW750236* MW750238* MW750239* MW750240*	MW838993* MW838992* MW838994* MW838995* MW838996*	MZ467043* — MW839000* MW839001* MZ467044*	this study this study this study this study this study
<i>G. zonatum</i>	FL-02 FL-03	FL, USA FL, USA	KJ143921 KJ143922	KJ143941 KJ143942	KJ143979 KJ143980	Zhou et al. 2015
<i>Tomophagus colossus</i>	TC-02	Vietnam	KJ143923	KJ143943	—	Zhou et al. 2015

*Newly generated sequences for this study. Bold font = new species.

ing the burn-in phase of the analyses, were discarded, while the remaining 1500 trees were used for calculating posterior probabilities in the majority rule consensus tree (the critical value for the topological convergence diagnostic is 0.01).

The phylogenetic tree was visualized with FigTree version 1.4.0 (Rambaut 2012) and made in Adobe Illustrator CS5 (Adobe Systems Inc., USA). Sequences derived in this study were deposited in GenBank (<http://www.ncbi.nlm.nih.gov>). The final sequence alignments and the phylogenetic trees are available at TreeBase (<http://www.treebase.org>, accession number: 28875).

Results

Phylogenetic analyses

The dataset composed of ITS, TEF1- α and RPB2 genes, comprising a total of 2092 characters including gaps, ITS (1–656 bp), TEF1- α (657–1192 bp) and RPB2 (1193–2092 bp), including 57 taxa with *Tomophagus colossus* (Fr.) C.F. Baker as the out-group taxon (Wang et al. 2009; Cao et al. 2012). Best model for the combined 3-gene dataset estimated and applied in the Bayesian analysis was GTR+I+G, lset nst = 6, rates = invgamma; prset statefreqpr = dirichlet (1,1,1,1). The phylogenetic analysis of ML and BI produce similar topology. The combined dataset analysis of RAxML generates a best-scoring tree (Figure 1), with the final ML optimization likelihood value of -13861.891117. The aligned matrix had 993 distinct alignment patterns, with 38.83% completely undetermined characters or gaps. The base frequency and rate are as follows: A = 0.215319, C = 0.266028, G = 0.260220, T = 0.258433; rate AC = 0.885915, AG = 5.586021, AT = 0.936363, CG = 1.205084, CT = 6.595971, GT = 1.000000; gamma distribution shape: α = 0.246210. Bootstrap support values with a maximum likelihood (ML) greater than 70%, and Bayesian posterior probabilities (BPP) greater than 0.95 are given above the nodes (Figure 1).

Phylogenetic analysis showed that five collections clustered together with high bootstrap support, forming a clade sister to *G. shanxiense* with strong bootstrap support (ML-BS = 96%, BPP = 1.00, Figure 1). Two other collections clustered with *G. aridicola*, *G. bambusicola*, *G. casuarinicola*, *G. calidophilum*, *G. enigmaticum* and *G. thailandicum* (ML-BS = 100%, BPP = 1.00), but forming as a distinct lineage.

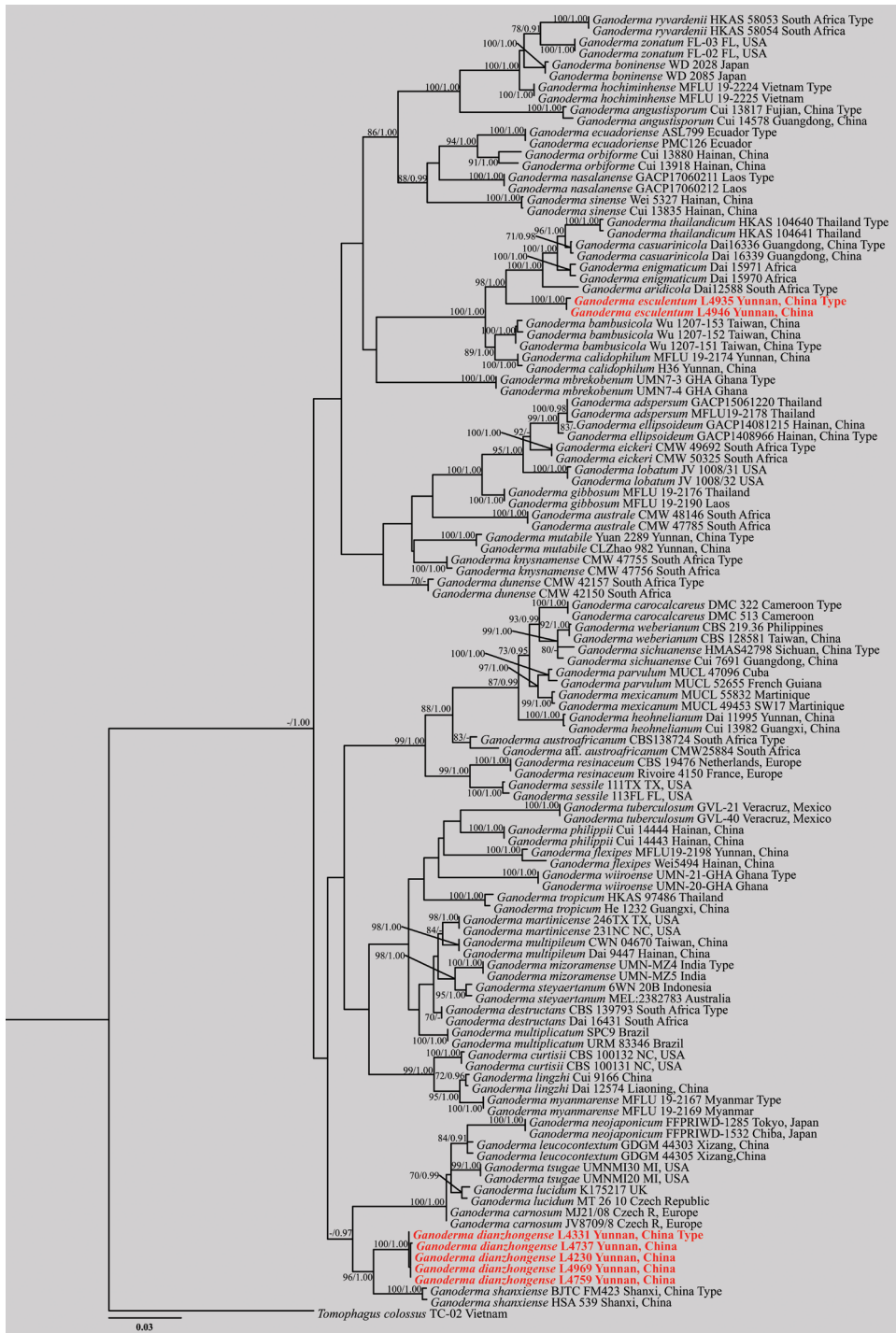


Figure 1. Phylogeny of the new *Ganoderma* species and related taxa based on ITS, TEF1- α and RPB sequence data. Branches are labeled with bootstrap values (ML) higher than 70%, and posterior probabilities (BPP) higher than 0.95. The new species are shown in bold red.

Taxonomy

Ganoderma dianzhongense J. He, H.Y. Su & S.H. Li, sp. nov.

Index Fungorum number: 558822

MycoBank No: 841408

Figure 2

Diagnosis. *Ganoderma dianzhongense* is characterized by its mesopodal basidiomata, oxblood red to violet brown pileus surface, melon seed kernel-shaped and broadly ellipsoid basidiospores.

Holotype. CHINA. Yunnan Province, Kunming City, Luquan County, on the rotten broad-leaved trees, alt. 2480 m, Shu-Hong Li, 8 Sept. 2016, L4331 (HKAS 110005).

Etymology. The epithet ‘dianzhong’ refers to central Yunnan province in Chinese, where the holotype was collected.

Description. **Basidiomata** annual, stipitate, sub-mesopodal to mesopodal or with the back sides fused, coriaceous to woody. **Pileus** single, suborbicular to reniform, up to 4.8–13.1 cm diam., 1.1 cm thick, weakly to strongly laccate, glossy and shiny, oxblood red (9E7) to violet brown (11F8), smooth, and covered by a thin hard crust, concentrically zonate or azonate. **Margin** distinct, slightly obtuse. **Stipe** 9.0–17.7 × 1.1–1.9 cm, central, cylindrical, strongly laccate, dark red brown (11C8) to purplish (14A8) or almost blackish red-brown (10F4), fibrous to woody. **Context** up to 0.4 cm thick, duplex; lower layer dark brown (8F8), fibrous, composed of coarse loose fibrils; upper layer putty (4B2); corky to woody, bearing distinct concentric growth zones, without black melanoid band. **Tubes** woody hard, grayish brown, up to 0.9 cm long, unstratified. **Pore** 4–6 per mm, round to angular, dissepiments slightly thick, entire; pore surface grey white to lead gray (2D2), turning light buff when dust (5D1).

Hypal system trimitic. Generative hyphae 2.0–3.5 µm in diameter, colorless, thin-walled, clamp connections present; skeletal hyphae 3.0–6.0 µm in diameter, subthick-walled to solid, non-septate, arboriform with few branches, yellowish to golden-yellow; binding hyphae 1–2.5 µm in diameter, thick-walled, frequently branched, interwoven, hyaline to yellowish, scarce; all the hyphae IKI–, CB+; tissues darkening in KOH.

Pileipellis a crustohymeniderm, cells 20–45 × 5.5–7.5 µm, clavate to cylindrical, entire or rarely with one lateral protuberance, thick-walled, without granulations in the apex, golden-yellow to yellowish-brown, thick-walled, moderately amyloid at maturity.

Basidiospores (80/6/3) (9.0) 10–**11.0**–12.0 (12.5) × (6.5) 7.0–**7.9**–8.5 (9.0) µm, $Q = (1.12) \ 1.25\text{--}1.55 \ (1.63)$, $Q_m = 1.40 \pm 0.09$ (including myxosporium); holotype: (40/2/1) 10.0–**10.9**–12 × 7.0–**7.9**–8.5 (9.0) µm, $Q = (1.20) \ 1.25\text{--}1.52$, $Q_m = 1.39 \pm 0.08$ (including myxosporium). mostly melon seed-shaped at maturity to broadly ellipsoid, usually with one end tapering and obtuse at maturity, with apical germ pore, yellowish to medium brown, IKI–, CB+, inamyloid; perispore wrinkled, double-walled, with coarse interwall pillars. **Basidia** widely clavate to utriform, hyaline, with a clamp connection and four sterigmata, 11–19 × 10–13 µm; basidioles pear-shaped to fusiform, 10–15 × 8–12 µm.

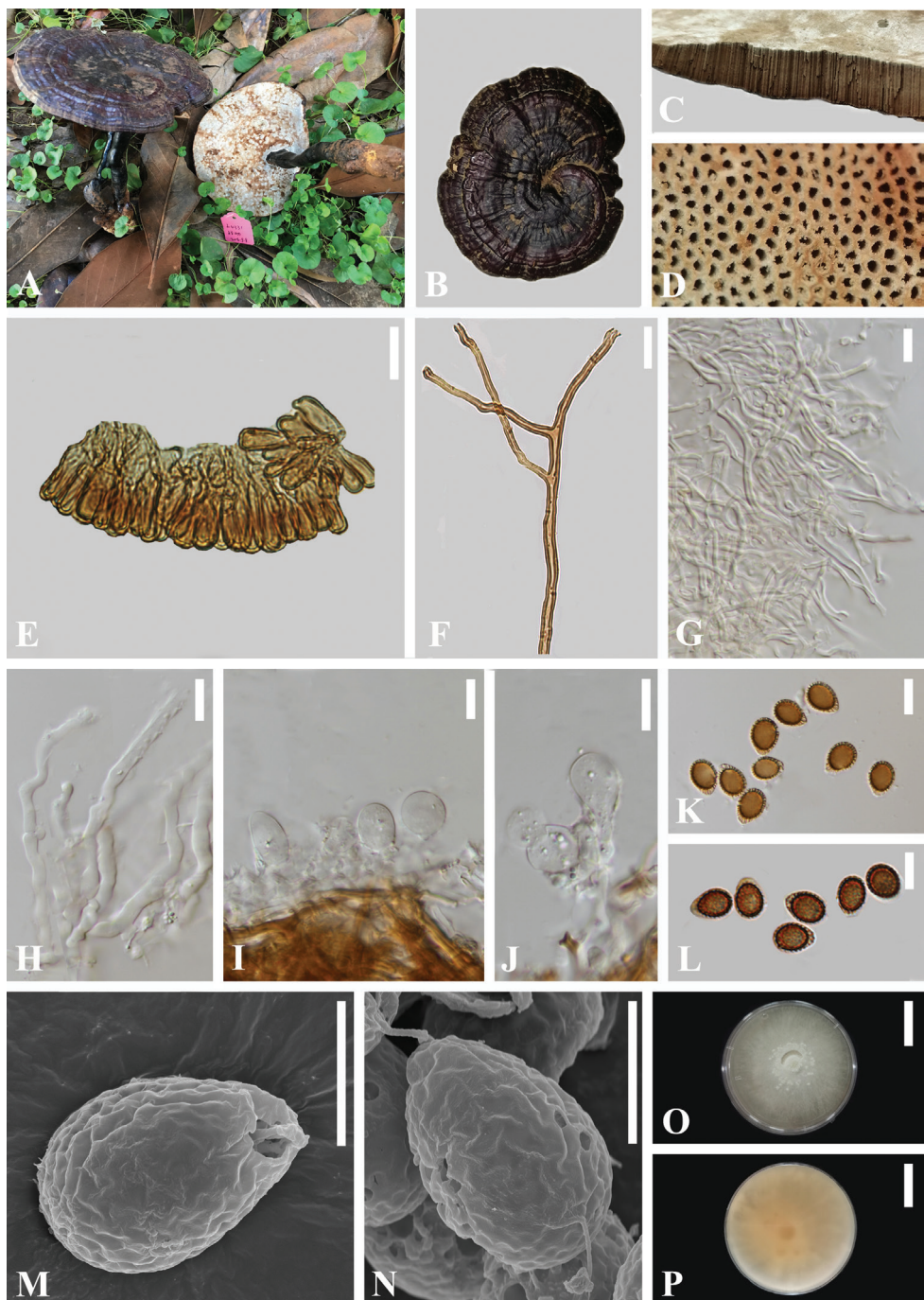


Figure 2. *Ganoderma dianzhongense* (HKAS 110005, holotype) **A** basidiomata **B** upper surface **C** cut side of pileus **D** pore surface **E** sections of pileipellis (LM) **F** skeletal hyphae from context (LM) **G** binding hyphae from tubes (LM) **H** generative hyphae from tubes (LM) **I-J** basidia and basidioles (LM) **K-L** basidiospores (LM) **M-N** basidiospores (SEM) **O-P** culture after incubation at 28 °C for 8 days. Scale bars: 20 mm (**O, P**); 10 µm (**E-L**); 5 µm (**M, N**). Photographs Jun He.

Habit. Scattered, during fall, decaying wood of broad-leaved trees including *Quercus* sp. Currently, only known from central Yunnan province, China.

Additional specimens examined. CHINA Yunnan province, Shilin County, alt. 2109m, Jun He, 28 Aug., 2019, L4969 (HKAS 112719); Songming County, alt. 2204m, Shu-Hong Li, 8 Jul., 2016, L4230 (HKAS 112716); Wuding County, alt. 2295m, Shu-Hong Li, 24 Jul., 2019, L4737 (HKAS 112717); ibid, alt. 2432m, Jun He, 26 Jul., 2019, L4759 (HKAS 112718).

***Ganoderma esculentum* J. He & S.H. Li, sp. nov.**

Index Fungorum number: 558823

MycoBank No: 841409

Figure 3

Diagnosis. *Ganoderma esculentum* is characterized by its strongly laccate chocolate brown pileus surface, slender stipe and narrow ellipsoid basidiospores.

Holotype. CHINA. Yunnan Province, Honghe City, Mengzi County, on a decaying wood log, alt. 1370 m, Jun He, 26 Aug., 2019, L4935 (HKAS 110006).

Etymology. The epithet ‘esculentum’ refers to this species named after a food.

Description. Basidiomata annual, stipitate, pleuropodal, laccate, woody-corky.

Pileus single, sub-orbicular to reniform to spathulate, up to 2.8–8.0 × 2.0–4.5 cm diam, 0.75 cm thick at the base, slightly convex to applanate; surface glabrous, rugose to radially rugose, strongly laccate, not cracking, with a hard crust, difficult to penetrate with the fingernail; surface brownish-black (6C8) to chocolate brown (6F4), almost homogeneous in the adult. **Margin** grayish orange(6B5) to concolorous, entire, acute to obtuse, smooth to sulcate. **Stipe** 10.0–17.5 × 0.5–1.0 cm, dorsally lateral to nearly dorsal, sub-cylindrical, solid, surface smooth, very shiny, dark brown (8F8) almost black, darker than pileus, fibrous to woody. **Context** up to 0.2 cm thick, composed of coarse loose fibrils, dark brown (8F8), with black melanoid band. **Tubes** 0.2–0.5 cm long, dark brown, woody hard, unstratified. **Pore** 5–8 per mm, circular or sub-circular, woody; pore surface white when fresh, darkening to soot brown(5F5) when aging and drying.

Hypal system trimitic. Generative hyphae 1.5–3.0 µm in diameter, colorless, thin-walled, clamp connections present; skeletal hyphae 3.5–5.5 µm in diameter, thick-walled to solid, non-septate, arboriform or not, non-branched or with a few branches in the distal end, golden brown; binding hyphae 1.0–3.0 µm in diameter, thick-walled, much-branched, arboriform, hyaline to yellowish, scarce; all the hyphae IKI–, CB+; tissues darkening in KOH.

Pileipellis a crustohymeniderm, cells 20–55 × 10–15 µm, narrowly clavate to tubular, generally smooth, slightly thick-walled to thick-walled with a wide lumen, occasionally expanded at the apex, without granulations, entire, yellowish to leather brown, weakly to strongly amyloid.

Basidiospores (40/3/2) (8.0) 9.0–**10.6**–12.5 × (5.0) 5.5–**6.6**–7.5 (8.0) µm, Q = (1.15) 1.34–**1.62**–2.01 (2.06), Q_m = 1.62±0.19 (including myxosporium); holo-



Figure 3. *Ganoderma esculentum* holotype (HKAS 110006) **A** basidiomata **B** upper surface **C** lower surface **D** cut side of pileus **E** pore surface **F** sections of pileipellis (LM) **G, H** skeletal hyphae from context (LM) **I** bingding hyphae from tubes (LM) **J** generative hyphae from tubes (LM) **K–M** basidiospores (LM) **N, O** basidiospores (SEM). Scale bars: 20 µm (**H**); 10 µm (**F, G, I–M**); 5 µm (**N, O**). Photographs Jun He.

type: (20/2/1) 9.0–**10.6**–12.5 × (5.0) 5.5–**6.5**–7.0 (8.0) µm, $Q = (1.34) 1.45$ –**1.64**–1.83 (2.06), $Q_m = 1.64 \pm 0.15$ (including myxosporium), narrow ellipsoid to truncate, slightly visible apical germ pore, brownish orange to light brown, IKI–, CB+, inamyloid; with a brown eusporium bearing fine, overlaid by a hyaline myxosporium, with interwall pillars. **Basidia** not observed.

Habit. On decaying hardwood trees or bamboo roots, accompanied in humus rich soil with over heavily rotted litter on the ground.

Additional specimens examined. CHINA. Yunnan province, Mengzi City, Xianansuo Town, alt. 1328m, Jun He, 26 Aug., 2019, L4946 (HKAS 112720).

Discussion

Ganodermataceae is a large family of polypores, and has received great attention from mycologists for over many decades. However, species identification and circumscriptions have been unclear and taxonomic segregation of the genera has been controversial because of different viewpoints among mycologists (Moncalvo et al. 1995; Moncalvo and Ryvarden 1997; Costa-Rezende et al. 2020). *Ganodermataceae* was treated as a synonym of *Polyporaceae* and classify the genus *Ganoderma* into *Polyporaceae* by Justo et al. (2017). Later, Cui et al. (2019) excluded *Ganoderma* from *Polyporaceae*, due to *Ganoderma* having unique double-walled basidiospores. In addition, recent studies have clarified someuncer-tainties of generic delimitation and classification of polypores with ganodermatoid basidiospores, and proved that *Ganodermataceae* is a monophyletic group (Costa-Rezende et al. 2020). More collections of this family are needed in order to estimate the attributes of this taxon better.

In the phylogenetic inferences, *Ganoderma dianzhongense* is sister to *G. shanxiense*, which is known from the northern Shanxi province in China (Figure 1). Morphologically, both species share similar characters of the mesopodal basidiomata, suborbicular to reniform pileus, and broadly ellipsoid basidiospores (Table 2). However, *G. shanxiense* differs from *G. dianzhongense* in having a red to reddish-brown pileus surface, wider basidiospores (11.0–13.0 × 8.0–9.5 µm), and narrower skeletal hyphae (2.5–5.0 µm, Liu et al. 2019).

Ganoderma dianzhongense resembles *G. sinense* and *G. orbiforme* in having suborbicular pileus (Table 2). However, *G. sinense* is characterized by wider basidiospores (9.5–13.4 × 7.0–10.2 µm) and slightly longitudinally crested basidiospores (Wang and Wu 2007) and a uniformly brown to dark brown context. *Ganoderma orbiforme* has a purplish black to light brown pileus, a variably brown context, irregularly digitated pileipellis cells, and ellipsoid to ovoid basidiospores (6.9–10.6 × 3.6–5.7 µm) with fine and short echinulae, and a subtropical to tropical distribution (Wang et al. 2014). *Ganoderma orbiforme* is also phylogenetically unrelated (Figure 1).

In our multi-locus phylogeny analysis (Figure 1), *G. aridicola*, *G. bambusicola*, *G. casuarinicola*, *G. calidophilum*, *G. enigmaticum*, *G. mbrekobenum*, *G. thailandicum* and *G. esculentum* formed a distinct lineage, and was clearly separated from other *Ganoderma* species. It is easy to distinguish them from the morphological characteristics. *Gano-*

Table 2. Morphological comparison of *Ganoderma dianzhongense* sp. nov., and *G. esculentum* sp. nov., with their closest relatives in the combined phylogeny.

Species	Shape	Context	Pileipellis cells	Pores	Basidiospores (μm)	Reference
<i>Ganoderma aridicola</i>	sessile dimidiate	context corky, fuscous, black melanoid band absent	moderately amyloid at maturity, $30\text{--}55 \times 5\text{--}8 \mu\text{m}$	6–8 per mm	$9.7\text{--}11.2 \times 7.0\text{--}7.8$	Xing et al. 2016
<i>G. bambusicola</i>	stipitate, reniform to semicircular	context fairly homogeneous, brownish, 1–2 mm thick	clavate or cylindrical, $35\text{--}65 \times 8\text{--}16 \mu\text{m}$	5–6 per mm	$11.0\text{--}12.5 \times 6.5\text{--}7.5$	Wu et al. 2020
<i>G. carnosum</i>	laterally to rarely eccentrically stipitate, dimidiate, orbicular to reniform	whitish and soft-corky context	amyloid elements up to $75 \mu\text{m}$ from clamp to the apex	3–4 per mm	$10.0\text{--}13 \times 7.0\text{--}8.5$	Patouillard 1889
<i>G. calidophilum</i>	stipitate, round or half-round	duplex context, 0.1–0.3 cm thick	—	4–6 per mm	$10.0\text{--}13.0 \times 6.2\text{--}8.7$	Zhao et al. 1979
<i>G. casuarinicola</i>	stipitate, sectorial to shell-shaped	context corky, black melanoid band absent.	moderately amyloid at maturity, $40\text{--}70 \times 5\text{--}13 \mu\text{m}$	4–6 per mm	$8.3\text{--}11.5 \times 4.5\text{--}7.0$	Xing et al. 2018
<i>G. dianzhongense</i>	stipitate, suborbicular to reniform	dark brown context, black melanoid band present	amyloid elements, $20\text{--}45 \times 5.5\text{--}7.5 \mu\text{m}$	5–8 per mm	$9.0\text{--}12.5 \times 6.5\text{--}9.0$	this study
<i>G. enigmaticum</i>	stipitate globular pileus	context soft, dark brown	amyloid elements $20\text{--}46 \times 5.5\text{--}9 \mu\text{m}$	3–5 per mm	$8.0\text{--}11.0 \times 3.5\text{--}6.0$	Coetzee et al. 2015
<i>G. esculentum</i>	stipitate, reniform to spathulate	dark brown context, without black melanoid bands	weakly to strongly amyloid, $20\text{--}55 \times 10\text{--}15 \mu\text{m}$	4–6 per mm	$8.0\text{--}12.5 \times 5.0\text{--}8.0$	this study
<i>G. kunmingense</i>	stipitate, spathulate or half-round	context wood color	—	4 per mm	$7.5\text{--}10.5 \times 6.0\text{--}9.0$	Zhao 1989
<i>G. lucidum</i>	stipitate to sessile	thinner context of white to slightly cream color context	amyloid hyphal end cells up to $7\text{--}11 \mu\text{m}$ diam	4–5 per mm	$7.7\text{--}11.5 \times 5.2\text{--}8.4$	Ryvarden and Gilbertson 1993
<i>G. leucocontextum</i>	stipitate, reniform to flabelliform	thinner context of white to slightly cream color	amyloid elements $30\text{--}60 \times 8\text{--}10 \mu\text{m}$	4–6 per mm	$9.5\text{--}12.5 \times 7.0\text{--}9.0$	Li et al. 2015
<i>G. mbrekobenum</i>	stipitate, maroon to liver brown	—	—	4–6 per mm	$8.0\text{--}11.5 \times 6.0\text{--}8.0$	Crous et al. 2016
<i>G. neojaponicum</i>	stipitate, reniform to suborbicular	0.5 cm thick, duplex	brownish orange, clavate like cells	3–5 per mm	$9.1\text{--}13.5 \times 5.7\text{--}8.9$	Imazeki et al. 1939
<i>G. orbiforme</i>	sessile, flabelliform or spathulate	context up to 0.4–1.0 cm thick, triplex	composed of apically acanthus like branched cells	4–6 per mm	$7.1\text{--}11.8 \times 5.2\text{--}7.7$	Ryvarden 2000
<i>G. sinense</i>	stipitate, dimidiate, suborbicular	soft and fibrous, dark brown	clavate like cells, dextrinoid	5–6 per mm	$9.5\text{--}13.8 \times 6.9\text{--}8.7$	Zhao 1979
<i>G. shanxiense</i>	stipitate, reniform to dimidiate	brown context	$25\text{--}30 \times 7.5\text{--}8.5 \mu\text{m}$	4–5 per mm	$11.0\text{--}13.0 \times 8.0\text{--}9.5$	Liu et al. 2019
<i>G. tsugae</i>	centrally to laterally stipitate, sub-dimidiate to dimidiate	whitish and soft corky context	$60\text{--}75 \times 7\text{--}10 \mu\text{m}$	4–6 per mm	$13.0\text{--}15.0 \times 7.5\text{--}8.5$	Murrill 1902
<i>G. thailandicum</i>	stipitate, greyish-red to brownish-red	context mostly brownish-red to reddish-brown	clavate to narrowly clavate, tuberculate	4–8 per mm	$6.8\text{--}10.2 \times 5.8\text{--}7.7$	Luangharn et al. 2019

derma bambusicola has a longer pileipellis ($35\text{--}65 \times 8\text{--}16 \mu\text{m}$) and wider basidiospores than those of *G. esculentum* ($10.0\text{--}13.0 \times 6.5\text{--}8.0 \mu\text{m}$, Wu et al. 2020). *Ganoderma aridicola* can be easily distinguished from *G. esculentum* by the sessile basidiomata and a fuscous to black pileus surface (Xing et al. 2016). *Ganoderma casuarinicola* differs from

G. esculentum by the latter has smaller basidiospores ($8.3\text{--}11.5 \times 4.5\text{--}7.0 \mu\text{m}$, Xing et al. 2018), grayish brown longer pores and sectorial to shell-shaped pileus. *Ganoderma enigmaticum* mainly differs from *G. esculentum* by its golden yellow pileus surface, narrower basidiospores ($8.0\text{--}11.0 \times 3.5\text{--}6.0 \mu\text{m}$, Coetzee et al. 2015) and causes root and butt rot of living and dead trees. *Ganoderma thailandicum* can be distinguished from *G. esculentum*, by its brownish-red pileus surface without radially rugose, narrowly clavate pileipellis cells with tuberculate and smaller basidiospores ($6.8\text{--}10.2 \times 5.8\text{--}7.7 \mu\text{m}$, Luangharn et al. 2019). *Ganoderma mbrekobennum* can be differentiated from *G. esculentum* by its woody to corky texture when dried, with ovoid basidiospores ($25.0\text{--}57.0 \times 6.0\text{--}12.0 \mu\text{m}$, Crous et al. 2016). *Ganoderma calidophilum* has a larger diameter binding hypha ($2.4\text{--}5.2 \mu\text{m}$) than *G. esculentum* ($1.0\text{--}3.0 \mu\text{m}$) and *G. calidophilum* has larger basidiospores ($7.3\text{--}14.6 \times 5.3\text{--}9.6 \mu\text{m}$, Zhao et al. 1979; Luangharn et al. 2021) than *G. esculentum* (including myxosporium).

Morphologically, *G. esculentum* resemble *G. kunmingense* by radially rugose, the pileus and slender stipe (Table 2). However, *G. kunmingense* has narrower hyphae, tissues not darkening in KOH, and broadly ellipsoid to sub-globose basidiospores ($7.5\text{--}10.5 \times 6.0\text{--}9.0 \mu\text{m}$, Zhao et al. 1989). In addition, *G. esculentum* shares also similarities with *G. neojaponicum* but the latter has a double-layered context with the paler layer near the pileus surface and wider basidiospores than those of *G. esculentum* ($9.1\text{--}13.5 \times 5.7\text{--}8.9 \mu\text{m}$, Imazeki et al. 1939; Hapuarachchi et al. 2019).

Acknowledgements

The authors thank Kunming Institute of Botany for providing the experimental platform. Dr Xiang-Hua Wang helped to analyze the molecular data and molecular lab work. We also thank Dr. Dan-Feng Bao and Hong-Wei Shen for their valuable suggestions on this study.

The research was financed by the National Natural Science Foundation of China (Project No. 31970021, 32060006), Yunnan Financial Special Project [YCJ (2020)323, 202102AE090036–05], Yunnan Science Technology Department and Technology Talents and Platform Program “Yunnan Province Technology Innovation Talents Training Objects” (Project ID 2017HB084) and Science and technology innovation and R&D promotion project of Qamdo City.

References

- Ahmadi K, Riazipour M (2007) Effect of *Ganoderma lucidum* on Cytokine Release by Peritoneal Macrophages. Iranian Journal of Immunology 4: 220–226.
- Bolaños AC, Bononi VLR, de Mello Gugliotta A (2016) New records of *Ganoderma multiplicatum* (Mont.) Pat. (Polyporales, Basidiomycota) from Colombia and its geographic distribution in South America. Check List 12: 1–7. <https://doi.org/10.15560/12.4.1948>

- Cabarroi-Hernández M, Villalobos-Arámbula AR, Torres-Torres MG, Decock C, Guzmán-Dávalos L (2019) The *Ganoderma weberianum-resinaceum* lineage: multilocus phylogenetic analysis and morphology confirm *G. mexicanum* and *G. parvulum* in the Neotropics. MycoKeys 59: 95–131. <https://doi.org/10.3897/mycokeys.59.33182>
- Cao Y, Wu SH, Dai YC (2012) Species clarification of the prize medicinal *Ganoderma* mushroom “Lingzhi”. Fungal Diversity 56: 49–62. <https://doi.org/10.1007/s13225-012-0178-5>
- Cao Y, Yuan HS (2013) *Ganoderma mutabile* sp. nov. from southwestern China based on morphological and molecular data. Mycological Progress 12: 121–126. <https://doi.org/10.1007/s11557-012-0819-9>
- Chan WK, Law HK, Lin ZB, Lau YL, Chan GC (2007) Response of human dendritic cells to different immunomodulatory polysaccharides derived from mushroom and barley. International Immunopharmacology 19: 891–899. <https://doi.org/10.1093/intimm/dxm061>
- Coetzee MP, Marincowitz S, Muthelo VG, Wingfield MJ (2015) *Ganoderma* species, including new taxa associated with root rot of the iconic *Jacaranda mimosifolia* in Pretoria, South Africa. IMA Fungus 6: 249–256. <http://doi.org/10.5598/imafungus.2015.06.01.16>
- Corner EJH (1983) Ad Polyporaceas I. *Amauroderma* and *Ganoderma*. Beihefte zur Nova Hedwigia, Weinheim.
- Costa-Rezende DH, Robledo GL, Goes-Neto A, Reck MA, Crespo E, Drechsler-Santos ER (2017) Morphological reassessment and molecular phylogenetic analyses of *Amauroderma* s.lat. raised new perspectives in the generic classification of the Ganodermataceae family. Persoonia 39: 254–269. <https://doi.org/10.3767/persoonia.2017.39.10>
- Costa-Rezende DH, Robledo GL, Drechsler-Santos ER, Glen M, Gates G, de Madrignac BR, Popoff OF, Crespo E, Góes-Neto A (2020) Taxonomy and phylogeny of polypores with ganodermatoid basidiospores (Ganodermataceae). Mycological Progress 19: 725–741. <https://doi.org/10.1007/s11557-020-01589-1>
- Crous PW, Wingfield MJ, Le Roux JJ, Richardson DM, Strasberg D, Shivas RG, Alvarado P, Edwards J, Moreno G, Sharma R, Sonawane MS, Tan Y-P, Altés A, Barasubiyé T, Barnes CW, Blanchette RA, Boertmann D, Bogo A, Carlavilla JR, Cheewangkoon R, Daniel R, de Beer ZW, de Jesús Yáñez-Morales M, Duong TA, Fernández-Vicente J, Geering ADW, Guest DI, Held BW, Heykoop M, Hubka V, Ismail AM, Kajale SC, Khemmuk W, Kolařík M, Kurli R, Lebeuf R, Lévesque CA, Lombard L, Magista D, Manjón JL, Marincowitz S, Mohedano JM, Nováková A, Oberlies NH, Otto EC, Paguigan ND, Pascoe IG, Pérez-Butrón JL, Perrone G, Rahi P, Raja HA, Rintoul T, Sanhueza RMV, Scarlett K, Shouche YS, Shuttleworth LA, Taylor PWJ, Thorn RG, Vawdrey LL, Vidal RS, Voitk A, Wong PTW, Wood AR, Zamora JC, Groenewald JZ (2015) Fungal Planet Description Sheets: 371–399. Persoonia 35: 264–327. <https://doi.org/10.3767/003158515X690269>
- Crous PW, Wingfield MJ, Richardson DM, Le Roux JJ, Strasberg D, Edwards J, Roets F, Hubka V, Taylor PWJ, Heykoop M, Martín MP, Moreno G, Sutton DA, Wiederhold NP, Barnes CW, Carlavilla JR, Gené J, Giraldo A, Guarnaccia V, Guarro J, Hernández-Restrepo M, Kolařík M, Manjón JL, Pascoe IG, Popov ES, Sandoval-Denis M, Woudenberg JHC, Acharya K, Alexandrova AV, Alvarado P, Barbosa RN, Baseia IG, Blanchette RA, Boekhout T, Burgess TI, Cano-Lira JF, Čmoková A, Dimitrov RA, Dyakov MYu, Dueñas M, Dutta

- AK, Esteve-Raventós F, Fedosova AG, Fournier J, Gamboa P, Gouliamova DE, Grebenc T, Groenewald M, Hanse B, Hardy GEStJ, Held BW, Jurjević Ž, Kaewgrajang T, Latha KPD, Lombard L, Luangsa-ard JJ, Lysková P, Mallátová N, Manimohan P, Miller AN, Mirabolfathy M, Morozova OV, Obodai M, Oliveira NT, Ordóñez ME, Otto EC, Paloi S, Peterson SW, Phosri C, Roux J, Salazar WA, Sánchez A, Sarria GA, Shin H-D, Silva BDB, Silva GA, Smith MTh, Souza-Motta CM, Stchige AM, Stoilova-Disheva MM, Sulzbacher MA, Telleria MT, Toapanta C, Traba JM, Valenzuela-Lopez N, Watling R, Groenewald JZ (2016) Fungal planet description sheets: 400–468. Persoonia 36: 316–458. <https://doi.org/10.3767/003158516X692185>
- Crous PW, Wingfield MJ, Burgess TI, Hardy GEStJ, Barber PA, Alvarado P, Barnes CW, Buchanan PK, Heykoop M, Moreno G, Thangavel R, van der Spuy S, Barili A, Barrett S, Caciola SO, Cano-Lira JF, Crane C, Decock C, Gibertoni TB, Guarro J, Guevara-Suarez M, Hubka V, Kolařík M, Lira CRS, Ordoñez ME, Padamsee M, Ryvarden L, Soares AM, Stchigel AM, Sutton DA, Vizzini A, Weir BS, Acharya K, Aloi F, Baseia IG, Blanchette RA, Bordallo JJ, Bratek Z, Butler T, Cano-Canals J, Carlavilla JR, Chander J, Cheewangkoon R, Cruz RHSF, da Silva M, Dutta AK, Ercole E, Escobio V, Esteve-Raventós F, Flores JA, Gené J, Góis JS, Haines L, Held BW, Jung MH, Hosaka K, Jung T, Jurjević Ž, Kautman V, Kautmanova I, Kiyashko AA, Kozanek M, Kubátová A, Lafourcade M, La Spada F, Latha KPD, Madrid H, Malysheva EF, Manimohan P, Manjón JL, Martín MP, Mata M, Merényi Z, Morte A, Nagy I, Normand AC, Paloi S, Pattison N, Pawłowska J, Pereira OL, Petterson ME, Picillo B, Raj KNA, Roberts A, Rodríguez A, Rodríguez-Campo FJ, Romański M, Ruszkiewicz-Michalska M, Scanu B, Schena L, Semelbauer M, Sharma R, Shouche YS, Silva V, Stanaszek-Kik M, Stielow JB, Tapia C, Taylor PWJ, Toome-Heller M, Vabeikhokhei JMC, van Diepeningen AD, Van Hoa N, Van Tri M, Wiederhold NP, Wrzosek M, Zothanzama J, Groenewald JZ (2017) Fungal Planet description sheets: 558–624. Persoonia 38: 240–384. <https://doi.org/10.3767/003158517X698941>
- Cui BK, Li HJ, Ji X, Zhou JL, Song J, Si J, Yang ZL, Dai YC (2019) Species diversity, taxonomy and phylogeny of Polyporaceae (Basidiomycota) in China. Fungal Diversity 97: 137–392. <https://doi.org/10.1007/s13225-019-00427-4>
- Dai YC, Yang ZL, Cui BK, Yu CJ, Zhou LW (2009) Species diversity and utilization of medicinal mushrooms and fungi in China. International Journal of Medicinal Mushrooms 11: 287–302. <https://doi.org/10.1615/IntJMedMushr.v11.i3.80>
- De Silva DD, Rapior S, Sudarman E, Stadler M, Xu J, Alias SA, Hyde KD (2013) Bioactive metabolites from macrofungi: ethnopharmacology, biological activities and chemistry. Fungal Diversity 62: 1–40. <https://doi.org/10.1007/s13225-012-0187-4>
- Donk MA (1948) Notes on Malesian fungi I. Bulletin du Jardin Botanique de Buitenzorg Série 317: 473–482.
- Douanla-Meli C, Langer E (2009) *Ganoderma carocalcareum* sp. nov., with crumbly-friable context parasite to saprobe on *Anthocleista nobilis* and its phylogenetic relationship in *G. resinaceum* group. Mycological Progress 8: 145–155. <https://doi.org/10.1007/s11557-009-0586-4>
- Doyle JJ, Doyle JL (1987) A rapid isolate procedure from small quantities of fresh leaf tissue. Phytochemical Bulletin 19: 11–15.

- Espinosa-García V, Mendoza G, Shnyreva VA, Padrón JM, Trigos Á (2021) Biological Activities of Different Strains of the Genus *Ganoderma* spp. (Agaricomycetes) from Mexico. International Journal of Medicinal Mushrooms 23:67–77. <https://doi.org/10.1615/IntJMed-Mushrooms.2021037451>
- Furtado JS (1981) Taxonomy of *Amauroderma* (Basidiomycetes, Polyporaceae). Mem N Y Bot Gard 34: 1–109.
- Glen M, Yuskianti V, Puspitasari D, Francis A, Agustini L, Rimbawanto A, Indrayadi H, Gafur A, Mohammed CL (2014) Identification of basidiomycete fungi in Indonesian hardwood plantations by DNA barcoding. Forest Pathology 44: 496–508. <https://doi.org/10.1111/efp.12146>
- Glez-Peña D, Gómez-Blanco D, Reboiro-Jato M, Fdez-Riverola F, Posada D (2010) ALTER: program-oriented conversion of DNA and protein alignments. Nucleic Acids Research 38: 14–18. <https://doi.org/10.1093/nar/gkq321>
- Hall TA (1999) BioEdit: a user-friendly biological sequence alignment editor and analysis program for Windows 95/98/NT. In: Nucleic Acids Symposium Series 41: 95–98.
- Hapuarachchi KK, Karunaratna SC, Phengsintham P, Yang HD, Kakumyan P, Hyde KD, Wen TC (2019) Ganodermataceae (Polyporales): Diversity in Greater Mekong Subregion countries (China, Laos, Myanmar, Thailand and Vietnam). Mycosphere 10: 221–309. <https://doi.org/10.5943/mycosphere/10/1/6>
- Hapuarachchi KK, Karunaratna SC, Raspé O, De Silva KHWL, Thawthong A, Wu XL, Kakumyan P, Hyde KD, Wen TC (2018) High diversity of *Ganoderma* and *Amauroderma* (Ganodermataceae, Polyporales) in Hainan Island, China. Mycosphere 9: 931–982. <https://doi.org/10.5943/mycosphere/9/5/1>
- He MQ, Zhao RL, Hyde KD, Begerow D, Kemler M, Yurkov A, McKenzie EHC, Raspé O, Kakishima M, Sánchez-Ramírez S, Vellinga EC, Halling R, Papp V, Zmitrovich IV, Buyck B, Ertz D, Wijayawardene NN, Cui BK, Schouteten N, Liu XZ, Li TH, Yao YJ, Zhu XY, Liu AQ, Li GJ, Zhang MZ, Ling ZL, Cao B, Antonín V, Boekhout T, da Silva BDB, Crop ED, Decock C, Dima B, Dutta AK, Fell JW, Geml J, Ghobad-Nejhad M, Giachini AJ, Gibertoni TB, Gorjón SP, Haelewaters D, He SH, Hodkinson BP, Horak E, Hoshino T, Justo A, Lim YW, Menolli JN, Mešić A, Moncalvo JM, Mueller GM, Nagy LG, Nilsson RH, Noordeloos M, Nuytinck J, Orihara T, Ratchadawan C, Rajchenberg M, Silva-Filho AGS, Sulzbacher MA, Tkalc̆ec Z, Valenzuela R, Verbeken A, Vizzini A, Wartchow F, Wei TZ, Weiß M, Zhao CL, Kirk PM (2019) Notes, outline and divergence times of Basidiomycota. Fungal Diversity 99: 105–367. <https://doi.org/10.1007/s13225-019-00435-4>
- Imazeki R (1939) Studies on *Ganoderma* of Nippon. Bulletin of the Tokyo Science Museum 1: 29–52.
- Justo A, Miettinen O, Floudas D, Ortiz-Santana B, Sjökvist E, Lindner DL, Nakasone K, Niemelä T, Larsson KH, Ryvarden L, Hibbett DS (2017) A revised family-level classification of the the Polyporales (Basidiomycota). Fungal Biology 121: 798–824. <https://doi.org/10.1016/j.funbio.2017.05.010>
- Karsten PA (1881) Enumeratio boletinearum et polyproearum fennicarum, systemate novo dispositarum. Revue de Mycologie 3: 16–19.

- Katoh K, Standley DM (2013) MAFFT multiple sequence alignment software Version 7: Improvements in performance and usability. *Molecular Biology and Evolution* 30: 772–780. <https://doi.org/10.1093/molbev/mst010>
- Kinge TR, Mih AM (2011) *Ganoderma ryvardenense* sp. nov. associated with basal stem rot (BSR) disease of oil palm in Cameroon. *Mycosphere* 2: 179–188.
- Kornerup A, Wanscher JH (1978) Methuen handbook of colour (3rd edn.) Methuen. London, England. <https://doi.org/10.1079/9780851998268.0000>
- Li TH, Hu HP, Deng WQ, Wu SH, Wang DM, Tsering T (2015) *Ganoderma leucocontextum*, a new member of the *G. lucidum* complex from southwestern China. *Mycoscience* 56: 81–85. <https://doi.org/10.1016/j.myc.2014.03.005>
- Liu H, Guo LJ, Li SL, Fan L (2019) *Ganoderma shanxiense*, a new species from northern China based on morphological and molecular evidence. *Phytotaxa* 406: 129–136. <https://doi.org/10.11646/phytotaxa.406.2>
- Liu YJ, Whelen S, Hall BD (1999) Phylogenetic relationships among ascomycetes: evidence from an RNA polymerase II subunit. *Molecular Biology and Evolution* 16: 1799–1808. <https://doi.org/10.1093/oxfordjournals.molbev.a026092>
- Loyd AL, Held BW, Barnes CW, Schink MJ, Smith ME, Smith JA, Blanchette RA (2018) Elucidating '*lucidum*': distinguishing the diverse laccate *Ganoderma* species of the United States. *PLoS ONE* 13: e0199738. <https://doi.org/10.1371/journal.pone.0199738>
- Luangharn T, Karunaratna SC, Dutta AK, Paloi S, Lian CK, Huyen LT, Pham HND, Hyde KD, Xu JC, Mortimer PE (2021) *Ganoderma* (Ganodermataceae, Basidiomycota) species from the Greater Mekong Subregion. *Journal of Fungi* 7: 1–83. <https://doi.org/10.3390/jof7100819>
- Luangharn T, Karunaratna SC, Khan S, Xu JC, Mortimer PE, Hyde KD (2017) Antibacterial activity, optimal culture conditions and cultivation of the medicinal *Ganoderma austral*, new to Thailand. *Mycosphere* 8: 1108–1123. <https://doi.org/10.5943/myco-sphere/8/8/11>
- Luangharn T, Karunaratna SC, Mortimer PE, Kevin DH, Xu JC (2019) Additions to the knowledge of *Ganoderma* in Thailand: *Ganoderma casuarinicola*, a new record; and *Ganoderma thailandicum* sp. nov. *MycoKeys* 59: 47–65. <https://doi.org/10.3897/mycokeys.59.36823>
- Matheny PB, Wang Z, Binder M, Curtis JM, Lim YW, Nilsson RH, Hughes KW, Petersen RH, Hofstetter V, Ammirati JF, Schoch C, Langer GE, McLaughlin DJ, Wilson AW, Crane PE, Frøslev T, Ge ZW, Kerrigan RW, Slot JC, Vellinga EC, Liang ZL, Aime MC, Baroni TJ, Fischer M, Hosaka K, Matsuura K, Seidl MT, Vaura J, Hibbett DS (2007) Contributions of *rpb2* and *tef1* to the phylogeny of mushrooms and allies (Basidiomycota, Fungi). *Molecular Phylogenetics and Evolution* 43: 430–451. <https://doi.org/10.1016/j.ympev.2006.08.024>
- Miller MA, Pfeiffer W, Schwartz T (2010) Creating the CIPRES Science Gateway for inference of large phylogenetic trees. *Proceedings of the Gateway Computing Environments Workshop (GCE)*, New Orleans, 8 pp. <https://doi.org/10.1109/GCE.2010.5676129>
- Moncalvo JM, Ryvarden L (1997) A nomenclatural study of the Ganodermataceae Donk. *Synopsis Fungorum* 11: 1–114.
- Moncalvo JM, Wang HF, Hsue RS (1995) Gene phylogeny of the *Ganoderma lucidum* complex based on ribosomal DNA sequences. Comparison with traditional taxonomic characters. *Mycological Research* 99: 1489–1499. [https://doi.org/10.1016/S0953-7562\(09\)80798-3](https://doi.org/10.1016/S0953-7562(09)80798-3)

- Murrill, WA (1902) The Polyporaceae of North America: I. The genus *Ganoderma*. Bull Torrey BotClub 29: 599–608. <https://doi.org/10.2307/2478682>
- Nylander JAA, Wilgenbusch JC, Warren DL, Swofford DL (2008) AWTY (are we there yet?): a system for graphical exploration of MCMC convergence in Bayesian phylogenetics. Bioinformatics 24: 581–583. <https://doi.org/10.1093/bioinformatics/btm388>
- Paterson RR (2006) *Ganoderma*— a therapeutic fungal biofactory. Phytochemistry 67: 1985–2001. <https://doi.org/10.1016/j.phytochem.2006.07.004>
- Patouillard N (1889) Le genre *Ganoderma*. Bulletin de la Société Mycologique de France 5: p64.
- Pilotti CA, Sanderson FR, Aitken AB, Armstrong W (2004) Morphological variation and豪strange of two *Ganoderma* species from Papua New Guinea. Mycopathologia 158: 251–265. <https://doi.org/10.1023/B:MYCO.0000041833.41085.6f>
- Rambaut A (2012) FigTree version 1.4.0. <http://tree.bio.ed.ac.uk/software/figtree/>
- Rannala B, Yang Z (1996) Probability distribution of molecular evolutionary trees: a new method of phylogenetic inference. Journal of molecular evolution 43: 304–311. <https://doi.org/10.1007/BF02338839>
- Richter C, Wittstein K, Kirk PM, Stadler M (2015) An assessment of the taxonomy and chemotaxonomy of *Ganoderma*. Fungal Diversity 71: 1–15. <https://doi.org/10.1007/s13225-014-0313-6>
- Ronquist F, Teslenko M, van der Mark P, Ayres DL, Darling A, Höhna S, Larget B, Liu L, SuchardMA, Huelsenbeck JP (2012) MrBayes 3.2: efficient Bayesian phylogenetic inference and model choice across a large model space. Systematic Biology 61: 539–542. <https://doi.org/10.1093/sysbio/sys029>
- Ryvarden L (2000) Studies in neotropical polypores 2: a preliminary key to neotropical species of *Ganoderma* with a laccate pileus. Mycologia 92: 180–191. <https://doi.org/10.2307/3761462>
- Ryvarden L (2004) Neotropical polypores part 1. Synop Fung 19: 1–227.
- Ryvarden L, Gilbertson RL (1993) European polypores. Part 1. *Abortiporus Lindtneria*. Synopsis Fungorum 6: 1–387.
- Song J, Xing JH, Decock C, He XL, Cui BK (2016) Molecular phylogeny and morphology reveal a new species of *Amauroderma* (Basidiomycota) from China. Phytotaxa 260: 47–56. <https://doi.org/10.11646/phytotaxa.260.1.5>
- Steyaert RL (1972) Species of *Ganoderma* and related genera mainly of the Bogor and Leiden Herbaria. Persoonia 7: 55–118.
- Sun YF, Costa-Rezende DH, Xing JH, Zhou JL, Zhang B, Gibertoni TB, Gates G, Glen M, Dai YC, Cui BK (2020) Multi-gene phylogeny and taxonomy of *Amauroderma* s. lat. (Ganodermataceae). Persoonia 44: 206–239. <https://doi.org/10.3767/persoonia.2020.44.08>
- Swofford DL (2003) PAUP*: phylogenetic analysis using parsimony (*and other methods). Sinauer Associates, Sunderland, Massachusetts. <http://ci.nii.ac.jp/naid/110002665463/>
- Tchoumi JMT, Coetze MPA, Rajchenberg M, Roux J (2019) Taxonomy and species diversity of *Ganoderma* species in the Garden Route National Park of South Africa inferred from morphology and multilocus phylogenies. Mycologia 111: 730–747. <https://doi.org/10.1080/00275514.2019.1635387>
- Tchoumi JMT, Coetze MPA, Rajchenberg M, Wingfield MJ, Roux J (2018) Three *Ganoderma* species, including *Ganoderma dunense* sp. nov., associated with dying *Acacia cyclops*

- trees in South Africa. *Australasian Plant Pathology* 47: 431–447. <https://doi.org/10.1007/s13313-018-0575-7>
- Tham LX, Hung NLQ, Duong PN, Hop DV, Dentinger BTM, Moncalvo J (2012) *Tomophagus cattienensis* sp.nov., an ew Ganodermataceae species from Vietnam: evidence from morphology and ITS DNA barcodes. *Mycological Progress* 11: 775–780. <https://doi.org/10.1007/s11557-011-0789-3>
- Wang DM, Wu SH (2007) Two species of *Ganoderma* new to Taiwan. *Mycotaxon* 102: 373–378.
- Wang DM, Wu SH, Su CH, Peng JT, Shih YH, Chen LC (2009) *Ganoderma multipileum*, the correct name for “*G. lucidum*” in tropical Asia. *Botanical Studies* 50: 451–458.
- Wang DM, Wu SH, Yao YJ (2014) Clarification of the concept of *Ganoderma orbiforme* with high morphological plasticity. *PLoS ONE* 9: e98733. <https://doi.org/10.1371/journal.pone.0098733>
- Wang DW, Wu SH (2010) *Ganoderma hoehnelianum* has priority over *G. shangsiense*, and *G. williamsianum* over *G. meijiangense*. *Mycotaxon* 113: 343–349. <https://doi.org/10.5248/113.343>
- Wang XH, Buyck B, Verbeken A, Hansen K (2015) Revisiting the morphologyand phylogeny of *Lactifluus* with three new lineages from southern China. *Mycologia* 107: 941–958. <https://doi.org/10.3852/13-393>
- White TJ, Bruns T, Lee S, Taylor J (1990) Amplification and direct sequencing of fungal ribosomal RNA genes for phylogenetics. In: Innis MA, Gelfand DH, Sninsky JJ, White TJ (Eds) PCR protocols: a guide to methods and applications. Academic, San Diego, New York, pp 315–322. <https://doi.org/10.1016/B978-0-12-372180-8.50042-1>
- Wu SH, Chern CL, Wei CL, Chen YP, Akiba M, Hattori T (2020) *Ganoderma bambusicola* sp. nov. (Polyporales, Basidiomycota) from southern Asia. *Phytotaxa* 451: 75–85. <https://doi.org/10.11646/phytotaxa.456.1.5>
- Xing JH, Song J, Decock C, Cui BK (2016) Morphological characters and phylogenetic analysis reveal a new species within the *Ganoderma lucidum* complex from South Africa. *Phytotaxa* 266: 115–124. <https://doi.org/10.11646/phytotaxa.266.2.5>
- Xing JH, Sun YF, Han YL, Cui BK, Dai YC (2018) Morphological and molecular identification of two new *Ganoderma* species on *Casuarina equisetifolia* from China. *MycoKeys* 34: 93–108. <https://doi.org/10.3897/mycokeys.34.22593>
- Zhao JD (1989) Studies on the Taxonomy of Ganodermataceae in China XI. *Acta Mycologica Sinica* 8: 25–34. [In Chinese]
- Zhao JD, Hsu LW, Zhang XQ (1979) Taxonomic studies on the subfamily Ganaderoideae of China. *Acta Mycologica Sinica* 19: 265–279. [In Chinese]
- Zhao JD, Zhang XQ (2000) Flora Fungorum Sinicorum 18. Ganodermataceae. Science Press, Beijing. [In Chinese]
- Zhaxybayeva O, Gogarten JP (2002) Bootstrap, Bayesian probability and maximum likelihood mapping: exploring new tools for comparative genome analyses. *BMC Genomics* 3: e4. <https://doi.org/10.1186/1471-2164-3-4>
- Zhou LW, Cao Y, Wu SH, Vlasák J, Li DW, Li MJ, Dai YC (2015) Global diversity of the *Ganoderma lucidum* complex (Ganodermataceae, Polyporales) inferred from morphology and multilocus phylogeny. *Phytochemistry* 114: 7–15. <https://doi.org/10.1016/j.phytochem.2014.09.023>

Supplementary material I

Phylogenetic sequence dataset

Authors: Jun He

Data type: phylogenetic data

Explanation note: Sequence data of three partial loci internal transcribed spaces region (ITS), RNA polymerase II subunit 2 (RPB2), and translation elongation factor 1-alpha (TEF1- α) were used in the phylogenetic analyses.

Copyright notice: This dataset is made available under the Open Database License (<http://opendatacommons.org/licenses/odbl/1.0/>). The Open Database License (ODbL) is a license agreement intended to allow users to freely share, modify, and use this Dataset while maintaining this same freedom for others, provided that the original source and author(s) are credited.

Link: <https://doi.org/10.3897/mycokeys.84.69449.suppl1>